Target tracking control system for multi-UAV maritime applications

Autor: **Miguel Guedes Félix**
Alferes Aluno no Mestrado Integrado na Especialidade de Engenharia Electrotécnica
Academia da Força Aérea, Sintra

Orientador: **Tiago Miguel Monteiro de Oliveira**
Academia da Força Aérea, Sintra

Coorientador: **Diogo Alexandre Oliveira Silva**
Academia da Força Aérea, Sintra

Abstract

The importance of Unmanned Aerial Vehicles (UAV) applications is becoming increasingly clear with every new year. While a lot of research has been done in the past, there are still several research areas, topics and applications to unveil and explore. The Air Force Academy Research Center (CIAFA) is working on a new modular control architecture for UAVs that allows for the reutilization of several modules such as trajectory control, computer vision, automatic learning and sensory data fusion, applied to a large spectrum of missions, which includes automatic landing or terrestrial target tracking based on computer vision. This thesis contributes to the formal implementation of a command and control architecture, to be used in search and target tracking missions in a maritime environment. The architecture was idealized in Santos (2021), using three main operating modes: search mode, target tracking mode and collision avoidance mode. Specifically, this dissertation contributes to the implementation of the target tracking mode of that architecture, in the same application scenario, considering that after detecting the target, this should be followed in a collaborative way. The main focus of this target tracking mode implementation is a controller that allows for a group of aircrafts to follow a circular path centered at the target coordinates and moves together with it, using the Moving Path Following (MPF) method (Oliveira, Aguiar, and Encarnação (2016) and Jain (2019)). In a first phase, the proposed control architecture is validated through numerical simulations, considering kinematic unicycle type model for the aircrafts and a simulated target. Next, a more realistic approach is adopted, with software in the loop simulations, using an open source model for the considered aircrafts dynamics. In this phase, specific software modules are developed for the considered control system, using an architecture based on Python, ROS, PX4 and Gazebo. Finally, after the implementation and validation of these simulations, a new feature is added: a target detection algorithm based on the received data from one of the UAVs onboard cameras to estimate the target's position and velocity, using an automatic detection module developed in Alves, Oliveira, Cruz, and Silva (2022). These simulation closes the implemented multi-UAV control loop system using a computer vision algorithm. The obtained results show the efficiency of the proposed method in a realistic computational simulation context, which allows for a quick transition to eventual flight tests.

Keywords: Flight coordination, Moving Path Following, Non-linear control, UAVs

1 Introduction

Up until the year of 2022, the Portuguese Air Force (FAP), more specifically, the Air Force Academy Research Centre (CIAFA), has been involved in several important research projects such as the PITVANT, PERSEUS, SUNNY, SEAGULL or FIREFRONT, all using unmanned aircrafts (see AFA (2022)). These mainly focused on the development of tools and added capabilities and in the designing, manufacturing and operation of Unmanned Aerial Vehicles (UAVs). Among the stated projects, the main publications include target tracking and path following for fixed wing UAVs (Oliveira, Aguiar, and Encarnação (2016) and Oliveira, Aguiar, and Encarnacao (2017)), computer vision (Marques, Bernardino, Cruz, and Bento (2014a), Marques, Bernardino, Cruz, and Bento (2014b) and Cruz and Bernardino (2015)), multidisciplinary design optimization (Felix, Gomes, and Suleman (2013)), micro and nano flapping-wing aerial vehicles (Armanini, Caetano, de Croon, de Visser, and Mulder (2016)) and reliability and airworthiness for small UAVs (Gonçalves, Sobral, and Ferreira (2016) and Gonçalves, Sobral, and Ferreira (2017)).

It is intended, with this thesis, to continue the work done in Santos (2021) and Alves et al. (2022), where a command and control system for multiple vehicles to work on maritime environments is developed. Specifically, Alves et al. (2022) implemented a new command and control architecture for low cost UAVs, using a hardware and software framework which includes, among others: Autopilot PX4 (PX4 (2022)), Robot Operating System (ROS)/MAVROS (ROS (2022)) and Open CV (OpenCV (2022)). As a sequence to that work, the formal implementation of a command and control architecture to be used in target search and tracking in maritime environment was idealized in Santos (2021) using three main modes: search mode, following mode and collision avoidance mode (see Figure 1). In that work, classic path following and trajectory tracking controllers were also implemented as a solution to the flight formation control for the search mode in maritime environment missions.

In this paper, it is intended to implement a control system that allows a group of N UAVs to follow in a coordinated way a target in a given environment, using a computer vision system to estimate the target's position. Regarding the use of multiple vehicles, one must answer the following problems: which geometry is the most suitable to solve the problem in

the target tracking phase; which control architecture should be implemented; Which motion control technique is the most suitable.

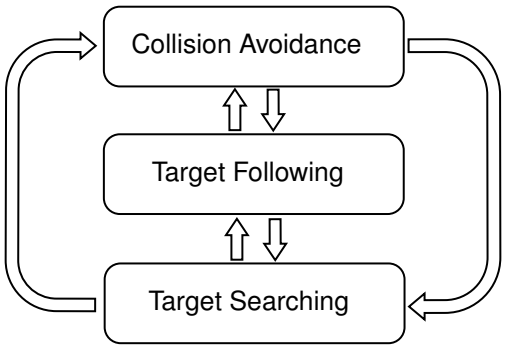

Figure 1: Control hierarchy defined in Santos (2021).

2 Literature Review

2.1 Multi-UAV Physical Architectures

Based on Maza, Ollero, Casado, and Scarlatti (2015) one possible scheme of classification for multi-UAV architectures is defined according to the coupling between the members. According to this classification, there are four types of couplings: physical coupling (see, for instance, Maza, Kondak, Bernard, and Ollero (2009) and Bernard, Kondak, Maza, and Ollero (2011)), formations (see, for instance Yun, Chen, Lum, and Lee (2010) and Paul, Krogstad, and Gravdahl (2008), with leader-follower and virtual leader approaches, respectively), swarms (see Rosalie et al. (2017) and Petrlik, Vonasek, and Saska (2019) for example applications) and intentional cooperation (see Viguria, Maza, and Ollero (2010), where coordination between aerial and ground vehicles is achieved and Han, hong Wang, and xing Yi (2013), for instance).

2.2 Control System Architectures

According to Ridao, Yuh, Batlle, and Sugihara (2000), control architecture is defined as the framework that manages both the sensors and actuators systems and thus enables the robot to undertake a user specified mission. Following Peng, Wang, Wang, and Han (2021), the control architecture can be divided into three main classifications: centralized control (examples can be found in Arrichiello, Chiaverini, and Fossen (2006) and Skjetne, Moi, and Fossen (2002)), decentralized control (see Liu, Wang, Peng, Chen, and Li (2019) and Dai, He, Lin, and Wang (2018)) and distributed control (see Peng, Wang, and Wang (2017) and Peng, Wang, Li, and Han (2020) for example implementations).

2.3 Vehicle Formation

There are different possible vehicle formations that define how these machines can interact with each other to accomplish a certain specified goal. In the literature, the main types are artificial potential functions (see Leonard and Fiorelli (2001) and Souza et al. (2022), for instance), graph-based methods (see Peng et al. (2017) and Peng, Wang, and Wang (2018)) and consensus based formations, which, according to Ren (2006), divides itself in the classical leader-follower (see Shojaei (2015) and Santos (2021), where this method was used for his control architecture implementation on a target search mission in maritime environments), virtual structure (see Skjetne et al. (2002), for instance) and behavioral approaches (see Hejase, Noura, and Drak (2015)). According to Peng et al. (2021), all these methods can be thought as classic motion-control problems, such as path following, trajectory tracking and target tracking.

2.4 Motion Control Techniques

To solve the problems stated above, different control techniques can be used such as Proportional- Integral-Derivative (PID), Linear-Quadratic Regulator (LQR) (B. Wang, Dong, and Chen (2010), Ratnoo, Sujit, and Kothari (2011) and Lee, Cho, and Kee (2010), for instance), gain scheduling (Cunha, Silvestre, and Pascoal (2003)), adaptive control (Kaminer et al. (2007) and Cao, Hovakimyan, Patel, Kaminer, and Dobrokhodov (2007)), sliding mode control (Nelson, Barber, McLain, and Beard (2007)), model predictive control (Li, Sun, and Oh (2010)) and Mansouri, Nikolakopoulos, and Gustafsson (2015)), backstepping (Chitrakaran, Dawson, Kannan, and Feemster (2006) and Ahmed and Subbarao (2010)) and Lyapunov vector fields (Frew, Lawrence, Dixon, Elston, and Pisano (2007)).

3 Flight Control System's Implementation

3.1 Proposed Solutions

By design, the MPF method (originally described in Oliveira, Aguiar, and Encarnacao (2016)) retains all the desirable characteristics of the classical path following method, namely smooth convergence to the moving path and the possibility of doing so at constant speed with respect to an inertial coordinate frame (Oliveira, Aguiar, and Encarnacao (2016)). Additionally, the MPF was successfully tested and validated in practical applications with CIAFA's UAVs. In this paper, the MPF controller that computes the inputs to steer the vehicle to the virtual particle point along the circular path is based on the work developed in Jain (2019), which extended the MPF problem (Oliveira, Aguiar, and Encarnacao (2016)). All the details regarding this Lyapunov-based controller, including the corresponding error dynamics derivation and proof of convergence are presented. The coordination system to get the vehicles equally spaced in the circle is performed by controlling the progression rate of the particle in the circle and having a leader and virtual particles to be followed, as done in Y. Wang, Wang, and Zhu (2019a). These particles are controlled to be equally spaced and to move along the path at a desired speed, being the control architecture applied separately from the vehicle steering control, in a chain like network. In order to follow the target, a circular path around it with a predefined constant radius is created since it is easy and simple to mathematically design and define a circular path and it is applicable to any number of vehicles (considering a minimum safe distance); also, fixed wing airborne vehicles can be always moving along this path, meaning that even when the target is steady, the aircraft still has a path to follow, never having the velocity going to zero. Furthermore, the UAVs are chosen to be equally spaced along the circle, which ensures a maximum distance between vehicles. Given the considered mission scenario in this thesis, where the UAVs should be flying relatively close to each other, it is assumed that a communication network connecting all the participating UAVs is available. Having shared data on the target between UAVs, possibly obtained by image acquisition and data fusion algorithms, can lead to better target estimates and better mission performances. Being so, a distributed architecture is implemented assuming that each vehicle knows the information about the vehicle that it is following, creating a chain communication network (Y. Wang, Wang, and Zhu (2019b)).

3.2 Mathematical Model and Control Laws

3.2.1 Problem Definition and Notation

Given, in two dimensions (see Figure 2), an inertial reference frame $\{I\}$ and a target frame $\{T\}$ attached to a moving target with unknown dynamics, let the position and velocity of this target be defined as $\mathbf{p}_t^I \in \Re^2$ and $\mathbf{v}_t^I \in \Re^2$, with respect to the inertial frame, respectively; it is assumed that in every time instant, these two variables are known. Let $\mathbf{p}_d^T : \Re \to \Re^2$ be a defined fixed reference geometric path parameterized by $\gamma \in \Re$, with $\dot{\gamma} \in \Re$ being the desired speed assignment. The parameter γ represents, for instance, the arc length along the path and it can be seen as a virtual particle along reference path. Being so, the speed of the virtual particle, $\dot{\gamma}$, dictates the evolution of this virtual particle along the path over time.

The vehicle kinematics are given by equations (1).

$$\begin{aligned} \dot{\mathbf{p}}_r^I(t) &= R_R^I(t)\mathbf{v}_r^R(t) \\ \dot{R_R^I}(t) &= R_R^I(t)S(\omega_r) \end{aligned} \tag{1}$$

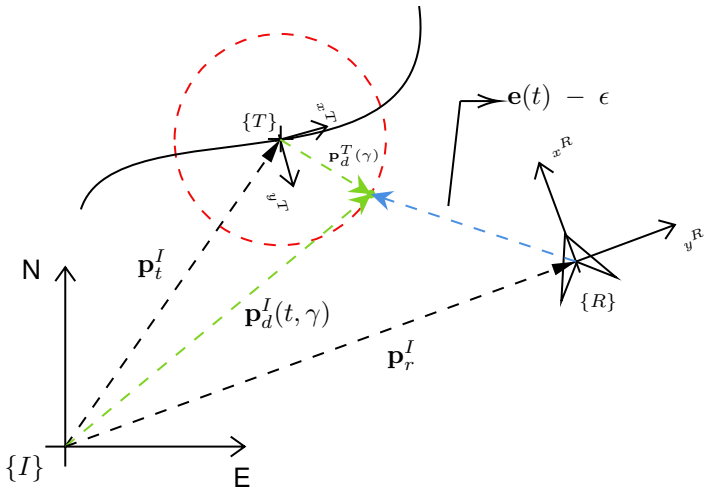

Figure 2: Coordinate frames, according to Jain (2019).

$\mathbf{p}_r^I \in \Re^2$ is the position of the vehicle expressed in the inertial frame, $\mathbf{v}_r^R = [v_f(t)\ 0]'$ is the linear velocity of the vehicle expressed in the robot body frame $\{R\}$ and $\omega_r(t)$ is the angular velocity of the vehicle. The two dimensional rotation matrix $R_R^I(t)$ represents the orientation of the vehicle frame $\{R\}$ with respect to the inertial frame of reference. The control input is defined as $\mathbf{u}(t) = [v_f\ \omega_r]'$ and is constrained, meaning that $v_{min} < v_f < v_{max}$ and $\omega_{min} < \omega_r < \omega_{max}$.

According to all the definitions stated above, the MPF problem can be stated as: given a trajectory $\mathbf{p}_t^I(t)$ with time derivative $\mathbf{v}_t^I$ and a desired geometric path $\mathbf{p}_d^T(\gamma)$ with desired speed $\dot{\gamma}$, the control problem is to design a control law for $\mathbf{u}(t)$ that steers the vehicle along the desired moving path $\mathbf{p}_d^I(t,\gamma) = \mathbf{p}_t^I + \mathbf{p}_d^T(\gamma)$ while satisfying the input constraints. Specifically, it is required to drive the term $||\mathbf{p}_r^I(t) - \mathbf{p}_d^I(t,\gamma)||$ towards an arbitrarily small neighborhood of the origin as $t \to \infty$.

3.2.2 Lyapunov-based Nonlinear Control Law

Following the definitions stated above, the error ($\mathbf{e}(t) = [\mathbf{e}_1\ \mathbf{e}_2]'$) can be defined as the difference between the current positions of the vehicle and the desired virtual particle to be followed, as $\mathbf{e}(t) = (R_R^I(t))'(\mathbf{p}_r^I(t) - \mathbf{p}_d^I(t,\gamma)) + \epsilon$, where ϵ is defined as a vector $\epsilon = [\epsilon_1\ \epsilon_2]'$ and it can be chosen to be arbitrarily small. By definition, the error is written with respect to the robot referential frame. The error dynamics are then defined in (2).

$$\dot{\mathbf{e}}(t) = (\dot{R}_R^I(t))'(\mathbf{p}_r^I(t) - \mathbf{p}_d^I(t,\gamma)) + (R_R^I(t))'(\dot{\mathbf{p}}_r^I(t) - \dot{\mathbf{p}}_d^I(t,\gamma)) \tag{2}$$

The terms $\mathbf{p}_d^I(t,\gamma) = \mathbf{p}_t^I(t) + \mathbf{p}_d^T(\gamma)$ and $\dot{\mathbf{p}}_d^I(t,\gamma) = \mathbf{v}_t^I(t) + \frac{\partial \mathbf{p}_d^T(\gamma)}{\partial \gamma}(\dot{\gamma})$ are the virtual particle position and its time derivative with respect to time, respectively.

Based on the definitions in (1) about the vehicle dynamics and the equations stated above, the error dynamics can now be rewritten as shown in (3).

$$\dot{\mathbf{e}}(t) = -S(\omega_r)\mathbf{e}(t) + \Delta\mathbf{u}(t) - (R_R^I(t))'\mathbf{v}_t^I(t) - (R_R^I(t))'\frac{\partial \mathbf{p}_d^T(\gamma)}{\partial \gamma}(\dot{\gamma}) \tag{3}$$

In the equation above, $\Delta = \begin{bmatrix} 1 & -\epsilon_2 \\ 0 & \epsilon_1 \end{bmatrix}$, where $\epsilon_1 \neq 0$ so that there is a direct control over the vehicle angular velocity.

The implemented control law based on Jain (2019) is represented in equation (4), where K_p is a constant known positive definite gain matrix and ϵ is defined such that the matrix Δ is invertible.

$$\mathbf{u}(t) = \Delta^{-1}(-K_p\mathbf{e}(t) + (R_R^I(t))'\mathbf{v}_t^I(t) + (R_R^I(t))'\frac{\partial \mathbf{p}_d^T(\gamma)}{\partial \gamma}\dot{\gamma}) \tag{4}$$

3.2.3 Virtual Particles Coordination

Now that a control law has been established to follow a given virtual particle in a desired moving path, the virtual particle needs to be defined so that coordination between vehicles is achieved. The coordination control law for controlling the rate of progression of the virtual particle along the parameterized path is based on the work done in Y. Wang et al. (2019b).

The control law implemented is presented in equation (5), where for each vehicle $i = 1, 2, ..., N$, $\tilde{\gamma}_i = \gamma_i - \gamma_{i-1} + \Delta_\gamma$ is the coordination error for vehicle i and Δ_γ is the desired along-path separation distance. $\beta \in \Re$ and $k_u \in \Re$ are positive constants. To achieve coordination, $\tilde{\gamma}_i \to 0$ must be assured as $t \to \infty$.

$$\dot{\gamma}_i = \dot{\gamma}_{i-1} - \beta \tanh(k_u \tilde{\gamma}_i) \tag{5}$$

It is assumed that there is a leader particle (particle number zero) that moves at a constant defined velocity (represented by $\dot{\gamma}_0$) along the parameterized path. The first particle is then controlled via the equation in (5) and followed by UAV one, and so forth for every particle and UAV.

This solution implies a consecutive share of information between UAVs, namely the γ and $\dot{\gamma}$ parameters, with a distributed control strategy. It is assumed that with this strategy, the necessary data is transmitted between UAVs, which is possible due to the fact that, in this flight phase, the UAVs are relatively close to each other.

Exponential error convergence to zero as time goes to infinity is assured for both presented control laws, based on Lyapunov methods (see Jain (2019) and Y. Wang et al. (2019b)).

The implementation is validated through numerical simulations with both a steady and a moving target. An unicycle type model was used to simulate the UAVs, in which the linear and angular velocity could be directly controlled. In the results, the errors converge to 0 as time goes to infinity, as expected, and the commanded control inputs achieve coordinated flight with the specified conditions.

4 Software In The Loop Simulations

An open source software framework was used to validate the command and control architecture implementation, in a more realistic setup with software in the loop simulations. The used software, includes, among others: Autopilot PX4 (PX4 (2022)), ROS/MAVROS (ROS (2022)), QGC (QGC (2022)) and Gazebo (Koenig and Howard (2004)). The final implemented ROS environment is depicted in Figure 14, which was done based on a modular approach with three main modules: particle controller, vehicle offboard controller and target data publishing module. Initially, the target data publishing module was implemented with a simple node that directly published the target data to all the UAVs in the flight formation, in a centralized manner. The results shown in this section refer to that implementation.

In all the presented results, the graphs are displayed with the vehicles correspondent colours: red refers to the first UAV, green to the second UAV and blue to the third UAV. The stars represent the UAVs starting positions and the circles the final positions, either for the UAVs or for the target. The starting positions for each one of them was chosen to be $\mathbf{p}^I_{r_1}(0) = [0;\ 2]$, $\mathbf{p}^I_{r_2}(0) = [0;\ 4]$ and $\mathbf{p}^I_{r_3}(0) = [0;\ 6]$ with the target starting at $\mathbf{p}^I_t(0) = [0;\ 0]$. The target's movement is defined as it was in the numerical simulations validation phase with the acceleration being given by $||\dot{\mathbf{v}}^I_t||(t) = 0.1\sin(0.07t)$ meters per second squared and the angular velocity governed by $\omega_t(t) = 0.02\cos(0.03t)$ radians per second (based on Oliveira, Aguiar, and Encarnacao (2016)). The remaining simulation properties were set to be the following: $K_p = [0.09\ 0; 0\ 0.005]$, $\beta = 0.2$, $k_u = 0.1$, $\epsilon = [10;\ 0]$, $\dot{\gamma}_0 = 15$ meters per second, $\gamma_i(0) = -i\Delta_\gamma$ meters, $r = 200$ meters, $\Delta_\gamma = \frac{2\pi r}{N}$ meters and N = 3. The control rate was set to 20 Hertz and the desired altitude was set to 30 meters.

In Figure 4, the UAVs converge and maintain themselves in the circular path, correctly following the target in a coordinated way. Figure 5 shows that after approximately 20 seconds, the UAVs converge to the desired altitude of 30 meters.

The errors plotted in Figures 6 and 7 converge to zero as time moves to infinity, as expected, similar to the results obtained in the numerical simulations.

Taking into account the presented results, it is safe to assume that the implementation is validated with the tracking errors converging to a value around zero and achieving a coordinated flight around a moving target, as desired. The next section explores the use of a computer vision system to obtain the target data.

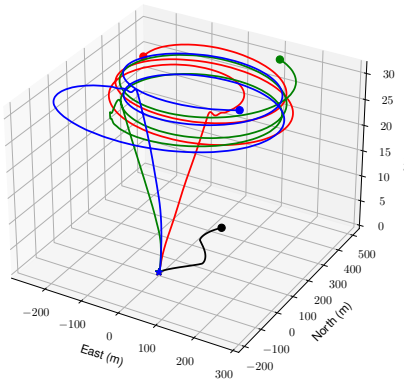

Figure 3: UAVs and target paths. The stars represent the UAVs starting positions and the circles the final positions.

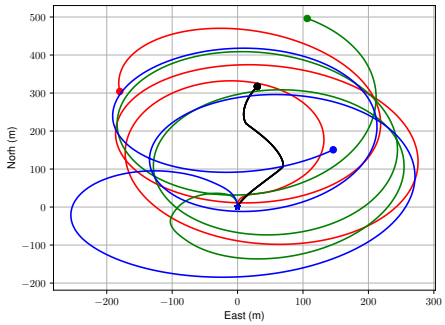

Figure 4: Longitudinal (North-East plane) perspective of the UAVs and target paths.

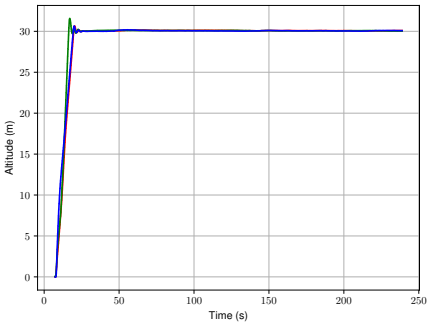

Figure 5: UAVs altitude (in meters) over time (in seconds).

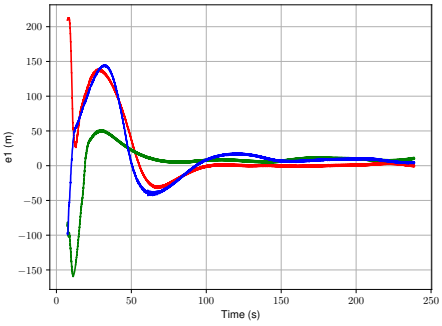

Figure 6: Error $\mathbf{e}_1$.

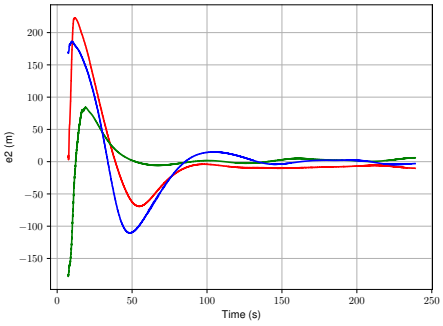

Figure 7: Error $\mathbf{e}_2$.

5 Closed Loop Simulations with Computer Vision

A new target detection computer vision algorithm is added (Alves et al. (2022)), to estimate the target velocity and positions based on acquired images through one of the UAVs onboard electro-optic sensor, as shown in the grey block in Figure 14.

The defined waypoints to control the target's movement were chosen to be the following: $\mathbf{p}_t^I(0) = [0;\ 0]$, $\mathbf{p}_t^I(50) = [0;\ 0]$, $\mathbf{p}_t^I(100) = [50;\ 0]$, $\mathbf{p}_t^I(150) = [150;\ 0]$, $\mathbf{p}_t^I(175) = [175;\ 0]$, $\mathbf{p}_t^I(200) = [250;\ 0]$, $\mathbf{p}_t^I(250) = [150;\ 0]$ and $\mathbf{p}_t^I(300) = [0;\ 0]$. The black line in Figure 8, Figure 9, Figure 10 and Figure 11 represents the target's estimated position while the magenta line indicates the target's real position.

From Figure 10 it is possible to visually conclude that the target estimations had a poor performance, with large estima-

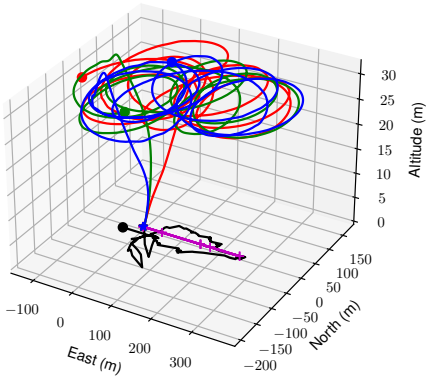

Figure 8: UAVs and target paths. The stars represent the UAVs starting positions and the circles the final positions. The target real position is depicted in magenta, where the magenta crosses represent the defined waypoints. The black line represents the computer vision system estimated target's position.

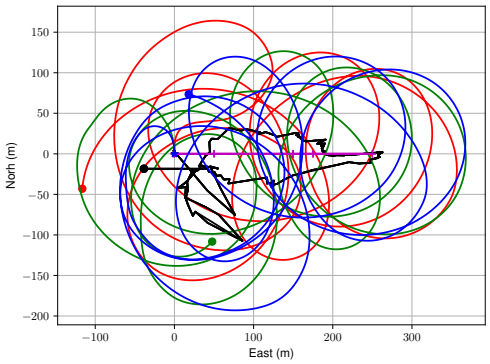

Figure 9: Longitudinal (North-East plane) perspective of the UAVs and target paths.

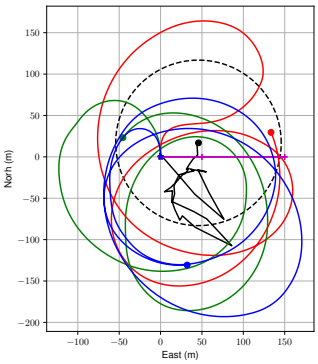

Figure 10: Longitudinal perspective at 100 seconds. The circles represent the last recorded positions.

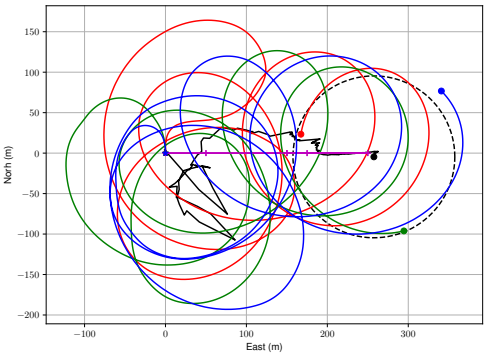

Figure 11: Longitudinal perspective at 200 seconds. The circles represent the last recorded positions.

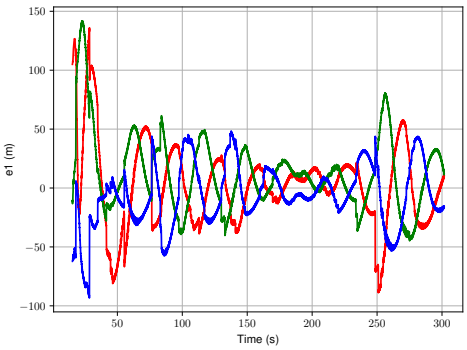

Figure 12: Error $\mathbf{e}_1$.

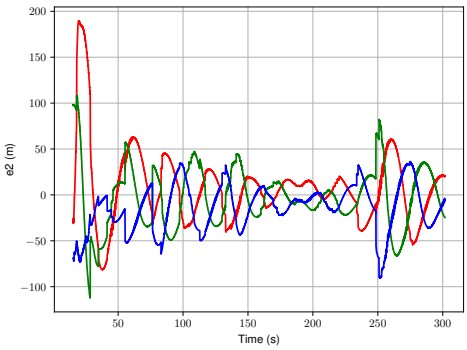

Figure 13: Error $\mathbf{e}_2$.

tion errors compared to the real target position. This is due to the fact that, during long periods of time, the UAV with the mounted camera could not capture the target on the acquired images. After the target is captured in the images and the UAVs start to correctly circling over it, the estimations start to get better and coordinated flight following the moving target is achieved. After 200 seconds, the target reaches its further most position and starts heading back to the origin, and its clear from Figure 11 that throughout this simulation period, the aircrafts followed in a coordinated way the moving target. Figure 9 show the UAVs full trajectory, where they headed back to the origin, correctly following once again the moving target. Regarding the errors plotted in Figures 12 and 13, although there is no clear convergence to 0, there is a tendency for lower error amplitudes as time goes forward. After 200 seconds, the target changes its movement to the opposite direction, and there is an increase in the error amplitude during approximately 50 seconds, after which it starts to decrease again, when the estimations stabilize and the target estimation algorithm correctly identifies the target direction change. Overall, the target could be followed in a coordinated way, proving the conjugation of a computer vision target position and velocity estimator with the proposed architecture. The results validate the implementation and the ultimate goal of following a moving target in a coordinated manner is once again achieved, this time with the added capability of real time estimation based on the acquired images from a simulated electro-optic sensor.

6 Conclusions

The developed work aimed to achieve the formal implementation of a command and control architecture to be used in search and target tracking missions in a maritime environment. After a thorough review of the available literature, several solutions are considered and the proposed solutions are justifiably chosen. The MPF method (Oliveira, Aguiar, and Encarnacao (2016) and Jain (2019)) using a distributed architecture with circular equidistant vehicle formation was implemented, achieving the design of a moving target tracking mode for the command and control architecture idealized in Santos (2021). The numerical simulations validated the implemented model, with overall satisfactory results and performance. In a more realistic approach, software in the loop simulations implemented the designed target tracking mode, achieving similar results and also validating the implementations. Lastly, a simulated electro-optic sensor onboard of one of the UAVs fed the obtained images to a computer vision algorithm (developed in Alves et al. (2022)) that estimated the target position and velocity, closing the control loop and validating the newly added capability through the shown results.

Future work can be developed in many different research areas to improve and continue this thesis. The developed target tracking mode can be integrated in the command and control architecture idealized in Santos (2021), with the other modes, which, in the case of the collision avoidance one, still needs to be developed. Future projects could focus on gimbaled camera systems, fusing the data obtained from all the UAVs to feed a computer vision algorithm. Overall, the written code is well documented, although some improvements could be made, namely by adding fail proof strategies and correcting code imposed limitations for scalability to a large number of UAVs. The investigation of different control laws, particularly to control the particle dynamics, could also be addressed to better adapt to different mission scenarios.

In the end, a coordinated control architecture was implemented with satisfactory results. With the proposed method and implementation, a number of aircrafts can follow a circular path around a generally moving target, while keeping a maximum distance between each other, as proved by the results presented throughout this dissertation.

References

AFA. (2022). *Portuguese Air Force Academy website.* From AFA - Academia da Força Aérea Portuguesa. Retrieved from `https://www.academiafa.edu.pt/`

Ahmed, M., & Subbarao, K. (2010, December). Nonlinear 3-D trajectory guidance for unmanned aerial vehicles. In *2010 11th international conference on control automation robotics & vision.* IEEE. Retrieved from `https://doi.org/10.1109/icarcv.2010.5707911` doi: 10.1109/icarcv.2010.5707911

Alves, J., Oliveira, T., Cruz, G., & Silva, D. (2022). *Software architecture for low-cost UAVs: an application considering automatic target tracking mission scenarios.* EasyChair Preprint no. 9143.

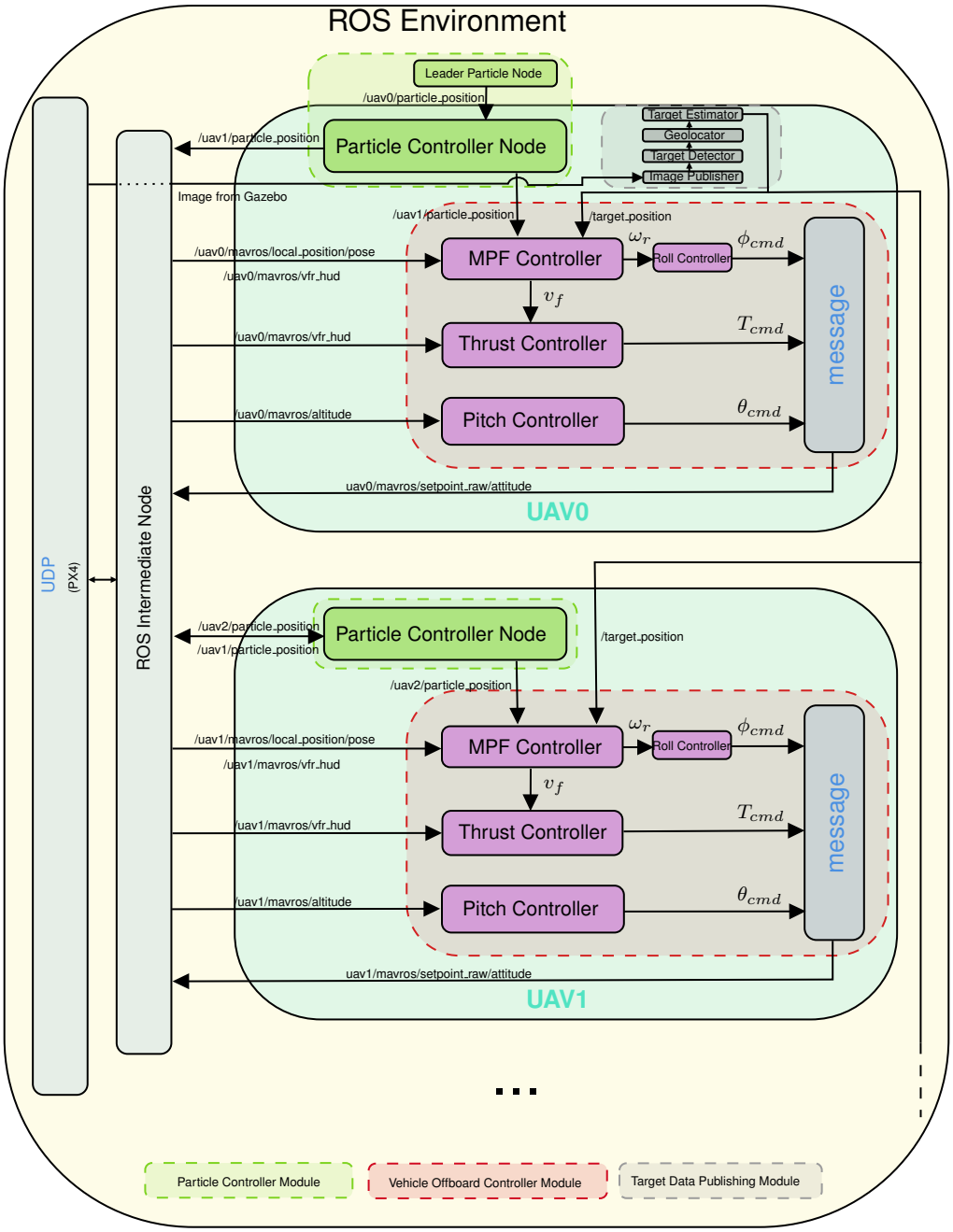

Figure 14: ROS environment with target detecting algorithm implemented in the target data publishing module.

Armanini, S. F., Caetano, J. V., de Croon, G. C. H. E., de Visser, C. C., & Mulder, M. (2016, June). Quasi-steady aerodynamic model of clap-and-fling flapping MAV and validation using free-flight data. *Bioinspiration & Biomimetics*, *11*(4), 046002. Retrieved from `https://doi.org/10.1088/1748-3190/11/4/046002` doi: 10.1088/1748-3190/11/4/046002

Arrichiello, F., Chiaverini, S., & Fossen, T. (2006). Formation control of marine surface vessels using the null-space-based behavioral control. In *Group coordination and cooperative control* (pp. 1–19). Springer-Verlag. Retrieved from `https://doi.org/10.1007/11505532_1` doi: 10.1007/11505532_1

Bernard, M., Kondak, K., Maza, I., & Ollero, A. (2011, October). Autonomous transportation and deployment with aerial robots for search and rescue missions. *Journal of Field Robotics*, *28*(6), 914–931. Retrieved from `https://doi.org/10.1002/rob.20401` doi: 10.1002/rob.20401

Cao, C., Hovakimyan, N., Patel, V., Kaminer, I., & Dobrokhodov, V. (2007, July). Stabilization of cascaded systems via l1 adaptive controller with application to a UAV path following problem and flight test results. In *2007 american control conference.* IEEE. Retrieved from `https://doi.org/10.1109/acc.2007.4283028` doi: 10.1109/acc.2007.4283028

Chitrakaran, V. K., Dawson, D. M., Kannan, H., & Feemster, M. (2006). Vision assisted autonomous path following for unmanned aerial vehicles. In *Proceedings of the 45th IEEE conference on decision and control.* IEEE. Retrieved from https://doi.org/10.1109/cdc.2006.377305 doi: 10.1109/cdc.2006.377305

Cruz, G., & Bernardino, A. (2015). Image saliency applied to infrared images for unmanned maritime monitoring. In *Lecture notes in computer science* (pp. 511–522). Springer International Publishing. Retrieved from https://doi.org/10.1007/978-3-319-20904-3_46 doi: 10.1007/978-3-319-20904-3_46

Cunha, R., Silvestre, C., & Pascoal, A. (2003, September). A path following controller for model-scale helicopters. In *2003 european control conference (ECC).* IEEE. Retrieved from https://doi.org/10.23919/ecc.2003.7085301 doi: 10.23919/ecc.2003.7085301

Dai, S.-L., He, S., Lin, H., & Wang, C. (2018, May). Platoon formation control with prescribed performance guarantees for USVs. *IEEE Transactions on Industrial Electronics*, *65*(5), 4237–4246. Retrieved from https://doi.org/10.1109/tie.2017.2758743 doi: 10.1109/tie.2017.2758743

Felix, L. F., Gomes, A., & Suleman, A. (2013, April). Topology optimization of a wing including self-weight load. In *54th AIAA/ASME/ASCE/AHS/ASC structures, structural dynamics, and materials conference.* American Institute of Aeronautics and Astronautics. Retrieved from https://doi.org/10.2514/6.2013-1869 doi: 10.2514/6.2013-1869

Frew, E. W., Lawrence, D. A., Dixon, C., Elston, J., & Pisano, W. J. (2007, July). Lyapunov guidance vector fields for unmanned aircraft applications. In *2007 american control conference.* IEEE. Retrieved from https://doi.org/10.1109/acc.2007.4282974 doi: 10.1109/acc.2007.4282974

Gonçalves, P., Sobral, J., & Ferreira, L. (2017, January). Establishment of an initial maintenance program for UAVs based on reliability principles. *Aircraft Engineering and Aerospace Technology*, *89*(1), 66–75. Retrieved from https://doi.org/10.1108/aeat-09-2014-0146 doi: 10.1108/aeat-09-2014-0146

Gonçalves, P., Sobral, J., & Ferreira, L. (2016). Reliability database for unmanned aerial vehicles based on morphological analysis. *The Aeronautical Journal*, *120*(1230), 1262–1274. doi: 10.1017/aer.2016.56

Han, J., hong Wang, C., & xing Yi, G. (2013, June). Cooperative control of UAV based on multi-agent system. In *2013 IEEE 8th conference on industrial electronics and applications (ICIEA).* IEEE. Retrieved from https://doi.org/10.1109/iciea.2013.6566347 doi: 10.1109/iciea.2013.6566347

Hejase, M., Noura, H., & Drak, A. (2015, 01). Formation flight of small scale unmanned aerial vehicles: A review. In (p. 221-248). doi: 10.1002/9781634827300ch10

Jain, R. P. K. (2019). *Decentralized cooperative control methods for multiple mobile robotic vehicles* (Unpublished master's thesis). Faculdade de Engenharia da Universidade do Porto.

Kaminer, I., Yakimenko, O., Dobrokhodov, V., Pascoal, A., Hovakimyan, N., Cao, C., ... Patel, V. (2007). *Coordinated path following for time-critical missions of multiple UAVs via l1 adaptive output feedback controllers.* Calhoun. Retrieved from https://calhoun.nps.edu/handle/10945/50330

Koenig, N., & Howard, A. (2004). Design and use paradigms for gazebo, an open-source multi-robot simulator. In *2004 ieee/rsj international conference on intelligent robots and systems (iros) (ieee cat. no.04ch37566)* (Vol. 3, p. 2149-2154 vol.3). doi: 10.1109/IROS.2004.1389727

Lee, S., Cho, A., & Kee, C. (2010, September). Integrated waypoint path generation and following of an unmanned aerial vehicle. *Aircraft Engineering and Aerospace Technology*, *82*(5), 296–304. Retrieved from https://doi.org/10.1108/00022661011092947 doi: 10.1108/00022661011092947

Leonard, N., & Fiorelli, E. (2001). Virtual leaders, artificial potentials and coordinated control of groups. In *Proceedings of the 40th ieee conference on decision and control (cat. no.01ch37228)* (Vol. 3, p. 2968-2973 vol.3). doi: 10.1109/CDC.2001.980728

Li, Z., Sun, J., & Oh, S. (2010, June). Handling roll constraints for path following of marine surface vessels using coordinated rudder and propulsion control. In *Proceedings of the 2010 american control conference.* IEEE. Retrieved from https://doi.org/10.1109/acc.2010.5531275 doi: 10.1109/acc.2010.5531275

Liu, L., Wang, D., Peng, Z., Chen, C. L. P., & Li, T. (2019, April). Bounded neural network control for target tracking of underactuated autonomous surface vehicles in the presence of uncertain target dynamics. *IEEE Transactions on Neural Networks and Learning Systems*, *30*(4), 1241–1249. Retrieved from https://doi.org/10.1109/tnnls.2018.2868978 doi: 10.1109/tnnls.2018.2868978

Mansouri, S. S., Nikolakopoulos, G., & Gustafsson, T. (2015, November). Distributed model predictive control for unmanned

aerial vehicles. In *2015 workshop on research, education and development of unmanned aerial systems (RED-UAS).* IEEE. Retrieved from https://doi.org/10.1109/red-uas.2015.7441002 doi: 10.1109/red-uas.2015.7441002

Marques, J. S., Bernardino, A., Cruz, G., & Bento, M. (2014a). An algorithm for the detection of vessels in aerial images. In *2014 11th ieee international conference on advanced video and signal based surveillance (avss)* (p. 295-300). doi: 10.1109/AVSS.2014.6918684

Marques, J. S., Bernardino, A., Cruz, G., & Bento, M. (2014b, August). An algorithm for the detection of vessels in aerial images. In *2014 11th IEEE international conference on advanced video and signal based surveillance (AVSS).* IEEE. Retrieved from https://doi.org/10.1109/avss.2014.6918684 doi: 10.1109/avss.2014.6918684

Maza, I., Kondak, K., Bernard, M., & Ollero, A. (2009). Multi-UAV cooperation and control for load transportation and deployment. In *Selected papers from the 2nd international symposium on UAVs, reno, nevada, u.s.a. june 8–10, 2009* (pp. 417–449). Springer Netherlands. Retrieved from https://doi.org/10.1007/978-90-481-8764-5_22 doi: 10.1007/978-90-481-8764-5_22

Maza, I., Ollero, A., Casado, E., & Scarlatti, D. (2015). Classification of multi-UAV architectures. In (chap. 38). Springer Science Business Media Dordrecht.

Nelson, D., Barber, D., McLain, T., & Beard, R. (2007, June). Vector field path following for miniature air vehicles. *IEEE Transactions on Robotics*, *23*(3), 519–529. Retrieved from https://doi.org/10.1109/tro.2007.898976 doi: 10.1109/tro.2007.898976

Oliveira, T., Aguiar, A. P., & Encarnacao, P. (2016, October). Moving path following for unmanned aerial vehicles with applications to single and multiple target tracking problems. *IEEE Transactions on Robotics*, *32*(5), 1062–1078. Retrieved from https://doi.org/10.1109/tro.2016.2593044 doi: 10.1109/tro.2016.2593044

Oliveira, T., Aguiar, A. P., & Encarnacao, P. (2017, May). Three dimensional moving path following for fixed-wing unmanned aerial vehicles. In *2017 IEEE international conference on robotics and automation (ICRA).* IEEE. Retrieved from https://doi.org/10.1109/icra.2017.7989315 doi: 10.1109/icra.2017.7989315

Oliveira, T., Aguiar, A. P., & Encarnação, P. (2016, June). A convoy protection strategy using the moving path following method. In *2016 international conference on unmanned aircraft systems (ICUAS).* IEEE. Retrieved from https://doi.org/10.1109/icuas.2016.7502567 doi: 10.1109/icuas.2016.7502567

OpenCV. (2022). *Opencv website.* From OpenCV. Retrieved from https://opencv.org/

Paul, T., Krogstad, T. R., & Gravdahl, J. T. (2008, October). Modelling of UAV formation flight using 3d potential field. *Simulation Modelling Practice and Theory*, *16*(9), 1453–1462. Retrieved from https://doi.org/10.1016/j.simpat.2008.08.005 doi: 10.1016/j.simpat.2008.08.005

Peng, Z., Wang, D., Li, T., & Han, M. (2020, June). Output-feedback cooperative formation maneuvering of autonomous surface vehicles with connectivity preservation and collision avoidance. *IEEE Transactions on Cybernetics*, *50*(6), 2527–2535. Retrieved from https://doi.org/10.1109/tcyb.2019.2914717 doi: 10.1109/tcyb.2019.2914717

Peng, Z., Wang, J., & Wang, D. (2017, April). Containment maneuvering of marine surface vehicles with multiple parameterized paths via spatial-temporal decoupling. *IEEE/ASME Transactions on Mechatronics*, *22*(2), 1026–1036. Retrieved from https://doi.org/10.1109/tmech.2016.2632304 doi: 10.1109/tmech.2016.2632304

Peng, Z., Wang, J., & Wang, D. (2018, May). Distributed maneuvering of autonomous surface vehicles based on neurodynamic optimization and fuzzy approximation. *IEEE Transactions on Control Systems Technology*, *26*(3), 1083–1090. Retrieved from https://doi.org/10.1109/tcst.2017.2699167 doi: 10.1109/tcst.2017.2699167

Peng, Z., Wang, J., Wang, D., & Han, Q.-L. (2021, February). An overview of recent advances in coordinated control of multiple autonomous surface vehicles. *IEEE Transactions on Industrial Informatics*, *17*(2), 732–745. Retrieved from https://doi.org/10.1109/tii.2020.3004343 doi: 10.1109/tii.2020.3004343

Petrlik, M., Vonasek, V., & Saska, M. (2019, October). Coverage optimization in the cooperative surveillance task using multiple micro aerial vehicles. In *2019 IEEE international conference on systems, man and cybernetics (SMC).* IEEE. Retrieved from https://doi.org/10.1109/smc.2019.8914330 doi: 10.1109/smc.2019.8914330

PX4. (2022). *PX4 user guide.* From PX4 User Guide. Retrieved from https://docs.px4.io/main/en/

QGC. (2022). *QGC website.* From QGC - QGroundControl - Drone Control. Retrieved from http://qgroundcontrol.com

Ratnoo, A., Sujit, P., & Kothari, M. (2011, January). Adaptive optimal path following for high wind flights. *IFAC Proceedings Volumes*, *44*(1), 12985–12990. Retrieved from https://doi.org/10.3182/20110828-6-it-1002.03720 doi: 10.3182/20110828-6-it-1002.03720

Ren, W. (2006). Consensus based formation control strategies for multi-vehicle systems. In *2006 american control conference.* IEEE. Retrieved from https://doi.org/10.1109/acc.2006.1657384 doi: 10.1109/acc.2006.1657384

Ridao, P., Yuh, J., Batlle, J., & Sugihara, K. (2000). On AUV control architecture. In *Proceedings. 2000 IEEE/RSJ international conference on intelligent robots and systems (IROS 2000) (cat. no.00ch37113).* IEEE. Retrieved from https://doi.org/10.1109/iros.2000.893126 doi: 10.1109/iros.2000.893126

ROS. (2022). *ROS website.* From ROS. Retrieved from https://www.ros.org/

Rosalie, M., Dentler, J. E., Danoy, G., Bouvry, P., Kannan, S., Olivares-Mendez, M. A., & Voos, H. (2017, June). Area exploration with a swarm of UAVs combining deterministic chaotic ant colony mobility with position MPC. In *2017 international conference on unmanned aircraft systems (ICUAS).* IEEE. Retrieved from https://doi.org/10.1109/icuas.2017.7991418 doi: 10.1109/icuas.2017.7991418

Santos, L. (2021). *Controlo de voo de formação para missões de busca em ambiente marítimo com UAVs* (Unpublished master's thesis). Academia da Força Aérea Portuguesa.

Shojaei, K. (2015, September). Leader–follower formation control of underactuated autonomous marine surface vehicles with limited torque. *Ocean Engineering*, *105*, 196–205. Retrieved from https://doi.org/10.1016/j.oceaneng.2015.06.026 doi: 10.1016/j.oceaneng.2015.06.026

Skjetne, R., Moi, S., & Fossen, T. (2002, December). Nonlinear formation control of marine craft. In *Proceedings of the 41st IEEE conference on decision and control, 2002.* (p. 1699—1704). IEEE. Retrieved from https://doi.org/10.1109/cdc.2002.1184765 doi: 10.1109/cdc.2002.1184765

Souza, R. M. J. A., Lima, G. V., Morais, A. S., Oliveira-Lopes, L. C., Ramos, D. C., & Tofoli, F. L. (2022, February). Modified artificial potential field for the path planning of aircraft swarms in three-dimensional environments. *Sensors*, *22*(4), 1558. Retrieved from https://doi.org/10.3390/s22041558 doi: 10.3390/s22041558

Viguria, A., Maza, I., & Ollero, A. (2010, January). Distributed service-based cooperation in aerial/ground robot teams applied to fire detection and extinguishing missions. *Advanced Robotics*, *24*(1-2), 1–23. Retrieved from https://doi.org/10.1163/016918609x12585524300339 doi: 10.1163/016918609x12585524300339

Wang, B., Dong, X., & Chen, B. M. (2010, June). Cascaded control of 3d path following for an unmanned helicopter. In *2010 IEEE conference on cybernetics and intelligent systems.* IEEE. Retrieved from https://doi.org/10.1109/iccis.2010.5518579 doi: 10.1109/iccis.2010.5518579

Wang, Y., Wang, D., & Zhu, S. (2019a). Cooperative moving path following for multiple fixed-wing unmanned aerial vehicles with speed constraints. *Automatica*, *100*, 82-89. Retrieved from https://www.sciencedirect.com/science/article/pii/S0005109818305363 doi: https://doi.org/10.1016/j.automatica.2018.11.004

Wang, Y., Wang, D., & Zhu, S. (2019b, February). Cooperative moving path following for multiple fixed-wing unmanned aerial vehicles with speed constraints. *Automatica*, *100*, 82–89. Retrieved from https://doi.org/10.1016/j.automatica.2018.11.004 doi: 10.1016/j.automatica.2018.11.004

Yun, B., Chen, B. M., Lum, K. Y., & Lee, T. H. (2010, January). Design and implementation of a leader-follower cooperative control system for unmanned helicopters. *Journal of Control Theory and Applications*, *8*(1), 61–68. Retrieved from https://doi.org/10.1007/s11768-010-9188-6 doi: 10.1007/s11768-010-9188-6